Cavity QED characterization of many-body atomic states in double-well potentials: Role of dissipation

W. Chen and P. Meystre

Department of Physics, B2 Institute, and College of Optical Sciences, The University of Arizona, Tucson, Arizona 85721, USA

(Received 31 October 2008; published 1 April 2009)

When an incident light beam is scattered off a sample of ultracold atoms trapped in a double-well potential, the statistical properties of the retroreflected field contain information about the quantum state of the atoms, and permit, for example, to distinguish between atoms in a superfluid state and a product of Fock states for each well (Mott-insulator-like state). This paper extends our previous analysis of this problem to include the effects of cavity damping. We use a Monte Carlo wave-function method to determine the two-time correlation function and time-dependent physical spectrum of the retroreflected field. We also analyze quantitatively the entanglement between the atoms and the light field for atoms in these two states.

DOI: 10.1103/PhysRevA.79.043801 PACS number(s): 42.50.Dv, 42.50.Nn, 37.10.Jk

I. INTRODUCTION

Ultracold atoms in optical lattices provide a remarkable test system in which to simulate a number of situations in condensed-matter physics [1] under exquisitely controlled conditions. The first example along these lines was the superfluid–to–Mott insulator transition [2,3] in bosonic systems, but the list of strongly correlated condensed-matter systems that can be simulated by atoms or molecules [4–7] in optical lattices has continued to grow since these pioneering experiments. Examples include, but are not limited, to the Bose-Hubbard and Fermi-Hubbard models [8,9], spin systems [10], and the Anderson lattice model [11]. In other examples, rotating lattices [12] are expected to lead to the realization of analogs of the quantum Hall effect, and random lattices have recently been used to study Anderson localization in atomic systems.

The ability to characterize the many-particle state of the atomic fields in optical lattices is of course central to the realization of these experiments [13]. In a recent paper [14], we proposed an optical scheme based on the diffraction of a quantized light field off the atomic sample to probe the number statistics of the matter-wave field. The basic idea is to use two light fields counterpropagating in a high-Q ring cavity and coupled via Bragg scattering off the atoms, a technique that is analogous to the Bragg reflection of x rays off a crystal, but operating in the quantum regime. We found that the dynamics of the light field strongly depends on the many-body state of the atomic field as well as on the well spacing. Specifically, the statistical properties of the Bragg-reflected light field for the atoms in each well in Fock states and for a superfluid—described both in terms of a number-conserving state and a mean-field coherent state—were found to provide a clear signature of the state of the atomic field.

The present paper extends these results to include the effects of cavity damping. We use a Monte Carlo wave-function method [15] to determine the two-time correlation functions and (time-dependent) physical spectrum [16] of the retroreflected field, restricting our considerations to the case of a simple two-well lattice. We also analyze quantitatively the entanglement [17] between the atoms and the light field for atoms in a product of Fock states and a superfluid state. Our main result is that even in the presence of dissipation, these quantities allow one to easily distinguish between these two states, and in addition permit one to decide between two familiar descriptions of that state.

Section II describes the main elements of our model, presenting in particular the effective non-Hermitian Hamiltonian required in the Monte Carlo wave-function simulations of the problem. The intensity reflected by the atoms via Bragg scattering is discussed in Sec. III, and Sec. IV presents the time-dependent physical spectrum of the reflected light. The quantum entanglement that may develop as a result of Bragg diffraction is quantified in Sec. V in terms of the logarithmic negativity. Finally, Sec. VI presents a conclusion and outlook.

II. MODEL

We consider a sample of ultracold bosonic two-level atoms [8] with transition frequency ω_a trapped in the lowest-energy state of a one-dimensional double-well potential [18,19] placed inside an optical ring resonator [20,21]. The atoms are driven by two counterpropagating cavity modes of wave vectors $\pm k$ and frequency $\omega_k = kc$; see Fig. 1. This interaction is described by the Hamiltonian

$$\hat{\mathcal{V}}_d = \int dx \hat{\psi}_e^\dagger(x)\langle e|\hat{\mathbf{d}}\cdot\hat{\mathbf{E}}(x)|g\rangle\hat{\psi}_g(x) + \text{H.c.}, \tag{1}$$

where $\hat{\mathbf{d}}$ is the dipole moment of the transition, $\hat{\mathbf{E}}(x)$ is the electric field operator, and $\hat{\psi}_e$ and $\hat{\psi}_g$ are field operators de-

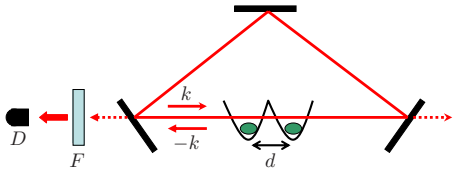

FIG. 1. (Color online) Atoms trapped in a double-well potential with well separation d and interacting with two counterpropagating modes with wave vectors $\pm k$ in a ring resonator. F: filter; D: detector.

scribing atoms in their excited and ground electronic states $|e\rangle$ and $|g\rangle$, respectively. We assume that the optical fields are sufficiently detuned from the atomic transition frequency ω_a that the excited electronic state can be adiabatically eliminated.

We proceed by expanding $\hat{\psi}_e$ and $\hat{\psi}_g$ as

$$\hat{\psi}_{e,g}(x) = \sum_m \psi_m^{(e,g)}(x)\hat{c}_m^{(e,g)}, \tag{2}$$

where $\hat{c}_m^{(e)}$ and $\hat{c}_m^{(g)}$ are the annihilation operators for excited- and ground-state atoms in the mth well, and $\psi_m^{(e)}$ and $\psi_m^{(g)}$ are the corresponding wave functions. Introducing also the operator

$$\hat{N}(d) = \hat{n}_0 + \hat{n}_1 e^{2ikd}, \tag{3}$$

where

$$\hat{n}_m \equiv \hat{c}_m^{(g)\dagger}\hat{c}_m^{(g)}, \tag{4}$$

and d is the well separation, the atom-field system is easily seen to be described by the Hamiltonian [14]

$$\hat{H} = \sum_k \hbar\omega_k \hat{a}_k^\dagger \hat{a}_k + \hbar g[\hat{N}(0)(\hat{a}_k^\dagger \hat{a}_k + \hat{a}_{-k}^\dagger \hat{a}_{-k}) + \hat{N}(d)\hat{a}_{-k}^\dagger \hat{a}_k + \hat{N}(-d)\hat{a}_k^\dagger \hat{a}_{-k}], \tag{5}$$

where a_k and $a_k^\dagger$ are bosonic annihilation and creation operators for mode k, and similarly for mode $-k$,

$$g = \frac{2\wp^2}{\Delta\hbar^2}\left|\int dx \mathcal{E}_{\pm k}(x)\psi_0^{(e)*}(x)\psi_0^{(g)}(x)\right|^2,$$

Δ is the detuning between the optical frequency and the frequency of the atomic transition, and $\wp$ is the dipole matrix element of that transition. We drop the label (g) in the following for notational clarity since no confusion is possible once the excited electronic state has been eliminated.

Cavity damping is treated in the usual way by coupling the cavity modes to a Markovian reservoir of harmonic oscillators of frequencies $\{\omega_q\}$, with the interaction Hamiltonian

$$\hat{\mathcal{V}}_r = \hbar(\hat{a}_k + \hat{a}_{-k})\sum_q g_q \hat{b}_q^\dagger + \text{H.c.} \tag{6}$$

Finally, the $+k$ cavity mode is driven by an oscillating classical current of amplitude η and frequency $\omega = \omega_k$,

$$\hat{\mathcal{V}}_p = \hbar\eta e^{-i\omega_k t}\hat{a}_k^\dagger + \text{H.c.} \tag{7}$$

The numerical studies that are the subject of this paper are conveniently carried out using a Monte Carlo wave-function approach [15]. In this case, the coupling of the system to the reservoir is described in terms of the effective non-Hermitian Hamiltonian

$$\hat{H}_{\text{eff}} = \hat{\mathcal{H}}_S - \frac{i\hbar}{2}\sum_{j=1,2}\hat{C}_j^\dagger \hat{C}_j, \tag{8}$$

where

$$\hat{C}_1 = \sqrt{2\gamma}\hat{a}_k, \quad \hat{C}_2 = \sqrt{2\gamma}\hat{a}_{-k} \tag{9}$$

and γ is the familiar Wigner-Weisskopf decay rate resulting from the coupling of the cavity modes to the Markovian reservoir. For the specific situation at hand this gives, in an interaction picture with respect to the Hamiltonian $\hat{H}_0 = \Sigma_k \hbar[\omega_k + g\hat{N}(0)]\hat{a}_k^\dagger \hat{a}_k$,

$$\hat{H}_{\text{eff}} = \hbar[g\hat{N}(d)a_{-k}^\dagger a_k + \eta\hat{a}_k^\dagger e^{ig\hat{N}(0)t} + \text{H.c.}] - i\hbar\gamma[\hat{a}_k^\dagger \hat{a}_k + \hat{a}_{-k}^\dagger \hat{a}_{-k}]. \tag{10}$$

III. REFLECTED INTENSITY

The light intensity transmitted and reflected by the trapped atoms depends strongly on the state of the atoms as well as on the well separation d. Throughout this paper we assume that the incident $+k$ mode is initially in a coherent state (with amplitude $\alpha = \sqrt{2}$ in our simulations) and the reflected $-k$ mode is in the vacuum state. Furthermore we concentrate on the special cases of well separations $d = \lambda/4$ and $\lambda/2$, for which the Hamiltonian $\hat{H}_{\text{eff}}$ becomes

$$\hat{H}_{\text{eff}}^{(\pm)} = \hbar g(\hat{n}_0 \pm \hat{n}_1)(a_{-k}^\dagger a_k + a_k^\dagger a_{-k}) + \hbar\eta(\hat{a}_k^\dagger e^{ig(\hat{n}_0+\hat{n}_1)t} + \text{H.c.}) - i\hbar\gamma(a_k^\dagger a_k + a_{-k}^\dagger a_{-k}). \tag{11}$$

Here the "plus" sign corresponds to the $d = \lambda/2$ case and the "minus" sign to the $d = \lambda/4$ case.

A. Fock states

When the atomic field has a well-defined number of atoms in each well, the system can be described by a product of Fock states. Atomic Fock states are eigenstates of effective Hamiltonian (11); that is, the operators $\hat{n}_0$ and $\hat{n}_1$ are constants of motion with eigenvalues n_0 and n_1, and it is possible to replace the operators by these eigenvalues in Eq. (11).

It is known [22] that if a system of coupled harmonic oscillators satisfies Heisenberg equations of motion that can be expressed as

$$\dot{\hat{a}}_j = F_j(\{\hat{a}_k(t)\}, t), \quad j = 1, \ldots, n, \tag{12}$$

where the functions F_j may depend explicitly on time, then if the oscillators are initially in a coherent state they will remain in a coherent state for all times. This is the case for the situation at hand. Hence the two modes of the light field are in coherent states whose amplitudes exhibit damped oscillations due to the combined effects of photon exchange between the incident and reflecting modes and of cavity decay. As to be expected, the oscillation frequency is proportional to the total number of atoms for the $d = \lambda/2$ case and to the difference in the populations of the two wells for $d = \lambda/4$. The difference between the oscillation frequencies in these two cases permits therefore a full determination of the well populations.

Figure 2 illustrates the time dependence of the reflected intensity for equal well populations and for the two special

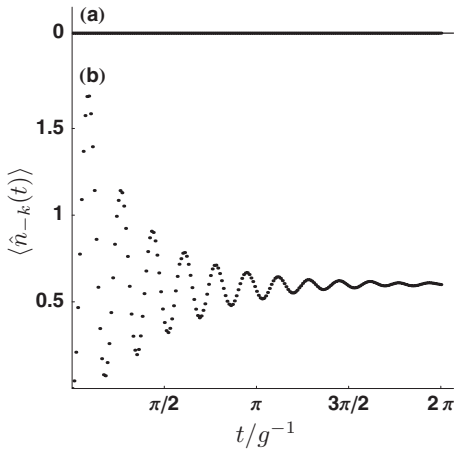

FIG. 2. Single trajectory [or average reflected intensities $\langle \hat{n}_{-k}(t) \rangle$] for atoms in the Fock states with three atoms per well for (a) $d=\lambda/4$ (zero signal) and (b) $d=\lambda/2$, $\eta=1.5g$, and $\gamma=0.9g$.

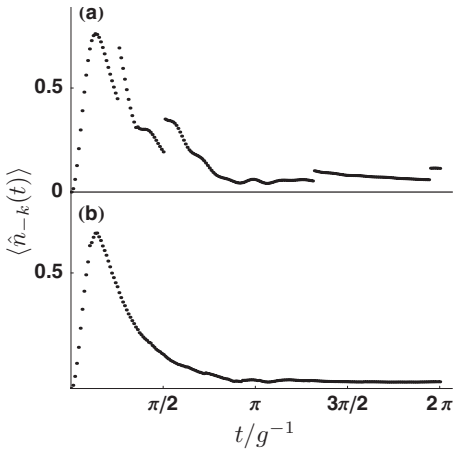

FIG. 3. Reflected intensity $\langle \hat{n}_{-k}(t) \rangle$ for atoms initially in the superfluid state $|\psi_{\mathrm{SF1}}\rangle$ with four atoms on average per well and $d=\lambda/4$. (a) Typical single trajectory. (b) Average over 100 trajectories, for $\eta=1.5g$ and $\gamma=0.9g$.

well separations. Different atomic populations in the two wells also result in an oscillating signal for the "destructive well separation" $d=\lambda/4$, but they are much weaker and slower than that in the "constructive case" $d=\lambda/2$. Since the light field remains in a coherent state at all times, the quantum jumps do not affect them and all Monte Carlo wave-function trajectories are identical in this case.

B. Superfluid

There are two particularly simple ways to approximate the state of the atoms in a superfluid state. The first one is essentially a mean-field approach that assumes that the atoms in the two wells are in coherent states,

$$|\psi_{\mathrm{SF1}}\rangle = |\alpha_0, \alpha_1\rangle = \sum_{n_0,n_1} c_{n_0,n_1} |n_0,n_1\rangle, \tag{13}$$

whereas the second description accounts for the fixed total number N of atoms and describes their state as

$$\begin{aligned} |\psi_{\mathrm{SF2}}\rangle &= \mathcal{N}^{-1}(c_1^\dagger + c_2^\dagger)^N |0,0\rangle \\ &= \sum_{n_0}^{N} \sqrt{\frac{N!}{2^N n_0!\,(N-n_0)!}} |n_0, N-n_0\rangle \\ &= \sum_{n_0}^{N} b_{n_0} |n_0, N-n_0\rangle. \end{aligned} \tag{14}$$

This subsection compares the reflected optical field corresponding to these two descriptions, assuming as before that the incident light field is initially in a coherent state and the reflected field is in a vacuum state.

Consider first the coherent-state description in Eq. (13). From the previous discussion we know that for fixed atom numbers in the two wells the state of the field remains a coherent state,

$$|\alpha,0;n_0,n_1\rangle \to |\alpha_k(n_0,n_1,d,t), \alpha_{-k}(n_0,n_1,d,t);n_0,n_1\rangle,$$

so that without quantum jumps between times 0 and t

$$|\psi(t)\rangle = \sum_{n_0,n_1} c_{n_0,n_1} |\alpha_k(n_0,n_1,d,t), \alpha_{-k}(n_0,n_1,d,t);n_0,n_1\rangle. \tag{15}$$

It is apparent from this expression that the atoms and the light field become entangled, a point to which we return in Sec. V. Also, since the optical field does not generally remain in a coherent state in this case, the quantum jumps resulting from the loss of photons due to dissipation become apparent in the single trajectories; see Fig. 3.

Comparing the present case to the situation in Sec. III A, we observe that there are no contributions to the backscattered intensity from situations with equal populations in the two wells, since the coupling between the incident and reflected fields is zero in these cases. Also, the oscillatory character of the backreflected light is now largely washed out by the uncertainty of the atom numbers in the two wells.

The number-conserving description [Eq. (14)] of the superfluid state leads to similar results, although the details of the dynamics are slightly different because of the fixed total number of atoms, which results in less atomic number uncertainty; see Fig. 4. In practice, it is therefore not expected that the backscattered intensity will allow one to unambiguously distinguish between the two descriptions.

IV. PHYSICAL SPECTRUM

We now turn to the analysis of the physical spectrum of the reflected optical field, which also provides a signature of the state of the atomic field.

Because the process under study is not stationary, the usual spectrum obtained from the Wigner-Khintchine theorem is not appropriate, and we use instead the time-dependent physical spectrum of Ref. [16]. We recall that this spectrum is defined as

$$\begin{aligned} S(t,\omega;\Gamma) = \int_0^t \int_0^t H^*(t-t_1,\omega,\Gamma) H(t-t_2,\omega,\Gamma) \\ \times \langle \hat{a}_{-k}^\dagger(t_1) \hat{a}_{-k}(t_2) \rangle dt_1 dt_2, \end{aligned} \tag{16}$$

where $H(t,\omega,\Gamma)$ is the response function of the filter, ω is its

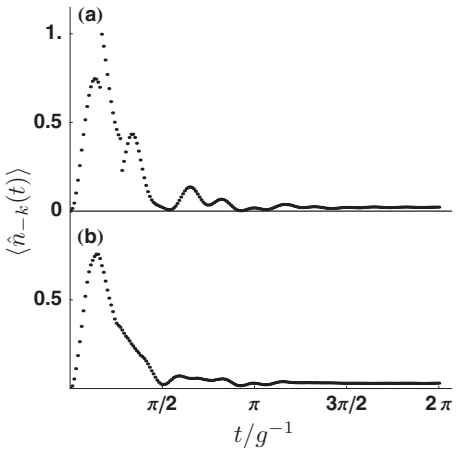

FIG. 4. Reflected intensity $\langle \hat{n}_{-k}(t) \rangle$ for atoms initially in the superfluid state $|\psi_{\mathrm{SF2}}\rangle$ with a total of eight atoms and $d=\lambda/4$. (a) Typical single trajectory; (b) average over 100 trajectories, for $\eta=1.5g$ and $\gamma=0.9g$.

setting frequency, and Γ is its bandwidth; see Fig. 1. Following Ref. [16], we assume that it is constant for the frequency range of interest, and choose the filter response function as

$$H(t,\omega;\Gamma) = \Theta(t)\Gamma e^{-(\Gamma+i\omega)t}, \tag{17}$$

where $\Theta(t)$ is the unit step function.

Figure 5 shows the real part of the two-time correlation function

$$G(t,t+\tau) = \langle \hat{a}^{\dagger}_{-k}(t)\hat{a}_{-k}(t+\tau)\rangle$$

for $d=\lambda/4$ and in the range $0 \le t+\tau \le T = 2\pi/g$ when the atoms in the two wells are in Fock states, while Fig. 6 shows that same function for the initial superfluid state $|\psi_{\mathrm{SF1}}\rangle$, and Fig. 7 for the initial superfluid state $|\psi_{\mathrm{SF2}}\rangle$. As was the case for the reflected intensity, the periodic oscillations of the reflected intensity characteristic of the Fock states case are washed out in the superfluid regime. Since the number-conserving description $|\psi_{\mathrm{SF2}}\rangle$ of the superfluid state corresponds to a smaller atom number uncertainty, the corresponding correlation function is characterized by stronger oscillations, intermediate between its description in terms of coherent states and the Fock states case; see Fig. 7.

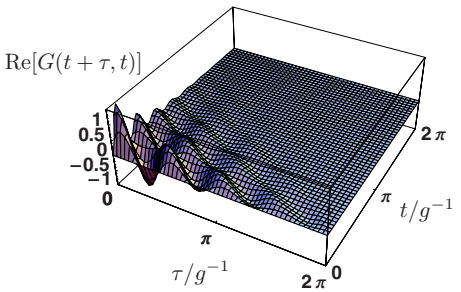

FIG. 5. (Color online) Two-time correlation function $G(t+\tau,t)$ in the Fock states case, with six atoms in well 0 and two in well 1. Well separation is $d=\lambda/4$, the pump constant is $\eta=0.1g$, and the decay constant is $\gamma=0.5g$.

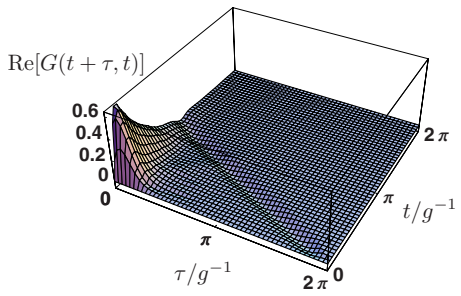

FIG. 6. (Color online) Two-time correlation function $G(t+\tau,t)$ for atoms initially in the superfluid state $|\psi_{\mathrm{SF1}}\rangle$ with a mean atom number of 4 per well and $d=\lambda/4$, $\eta=0.1g$, and $\gamma=0.5g$. The curve is the average over 50 trajectories at time t and 3 trajectories at time τ.

In terms of $\tau=t_1-t_2$, the physical spectrum $S(t,\omega;\Gamma)$ may be re-expressed as

$$\begin{aligned} S(t,\omega,\Gamma) &= 2\Gamma^2 e^{-2\Gamma t}\int_0^t d\tau e^{(\Gamma-i\omega)\tau} \\ &\quad \times \int_0^{t-\tau} dt_2 e^{2\Gamma t_2}\,\mathrm{Re}[\langle \hat{a}^{\dagger}_{-k}(t_2+\tau)\hat{a}_{-k}(t_2)\rangle] \\ &\equiv 2\Gamma^2 e^{-2\Gamma t} S_0(\omega,\Gamma), \end{aligned} \tag{18}$$

with $\tau \ge 0$.

Figure 8 shows the real part of $S_0(\omega)$ for atoms initially in a product of Fock states, while Figs. 9 and 10 are for atoms initially in superfluid states. In Fig. 8, the temporal oscillations of the correlation function $G(t+\tau,t)$ translates into a modulation of the Lorentzian spectrum due to the filter function at the oscillation frequency $\omega_- \equiv g|n_0-n_1|$ between the incident and reflected light fields. The physical spectrum provides therefore a direct measure of the population difference between the two wells for $d=\lambda/4$, of their sum for $d=\lambda/2$, and hence of n_0 and n_1 separately, i.e.,

$$\omega_{\pm} = g(n_0 \pm n_1),$$

$$n_{0,1} = (\omega_+ \pm \omega_-)/2g, \tag{19}$$

where we assumed $n_0 > n_1$ for concreteness. The second small dip at frequency $g(n_0+n_1)$ originates from the pump

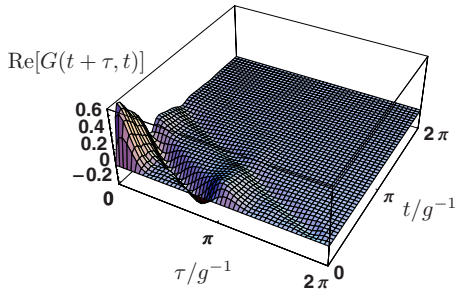

FIG. 7. (Color online) Two-time correlation function $G(t+\tau,t)$ for atoms initially in the superfluid state $|\psi_{\mathrm{SF2}}\rangle$ with a total number of eight atoms, $d=\lambda/4$, $\eta=0.1g$, and $\gamma=0.5g$. The curve is over 50 trajectories at time t and 3 trajectories at time τ.

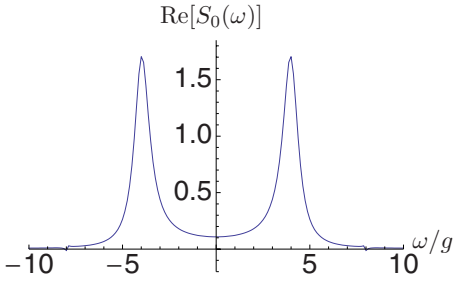

FIG. 8. (Color online) Real part of $S_0(\omega)$ for a Mott insulator state with six atoms in well 0 and two atoms in well 1, with $d=\lambda/4$. The peak is centered at $|n_0-n_1|$ in this case.

term, $\hbar\eta(\hat{a}_k^\dagger e^{ig(\hat{n}_0+\hat{n}_1)t}+\text{H.c.})$, in Hamiltonian (11).

Figures 9 and 10 show the physical spectra for the coherent and number-conserving superfluid states $|\psi_{\text{SF1}}\rangle$ and $|\psi_{\text{SF2}}\rangle$, respectively. In the number-conserving description [Eq. (14)], the total atom number N is fixed. Hence for $d=\lambda/4$ the population difference between the two wells, $|2n_0-N|$, can only take all even or all odd numbers, depending on N. This restriction disappears in the coherent-state description of $|\psi_{\text{SF1}}\rangle$, so that additional peaks appear although the mean number of atoms in each well is the same in Figs. 9 and 10.

We conclude this discussion by mentioning that for a well separation $d=\lambda/2$ case the superfluid descriptions $|\psi_{\text{SF1}}\rangle$ and $|\psi_{\text{SF2}}\rangle$ result in completely different spectra. For $|\psi_{\text{SF1}}\rangle$ the spectrum is similar to that of the $d=\lambda/4$ case since n_0 and n_1 are independent and hence give all combinations of different total numbers (n_0+n_1) to form the spectrum. By contrast, the number-conserving description $|\psi_{\text{SF2}}\rangle$ results in a single sharp peak, just as in the Fock states case; see Fig. 8.

Next we use the number-conserving approximation $|\psi_{\text{SF2}}\rangle$ to investigate the relation between the full width at half maximum (FWHM) of the physical spectrum and the atomic number uncertainties in the two wells. We evaluate that width with the help of an envelope function fitted in the way illustrated in Fig. 11. The atomic number uncertainties σ are defined in the usual way as

$$\sigma = \sqrt{\sum_{m=0}^{N} (m-\bar{m})^2 b_m^2}, \tag{20}$$

where $\bar{m}=\Sigma_m m b_m^2$, N is the total number of atoms, and b_m^2, the probability of having m atoms in one of the wells, is a

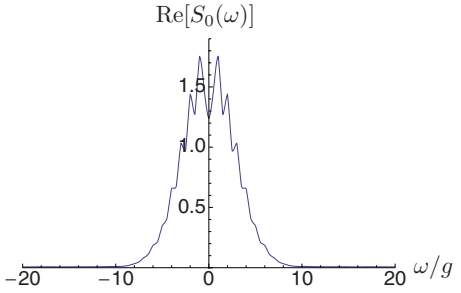

FIG. 9. (Color online) Real part of $S_0(\omega)$ of superfluid states $|\psi_{\text{SF1}}\rangle$ with each well containing four atoms on average and $d=\lambda/4$.

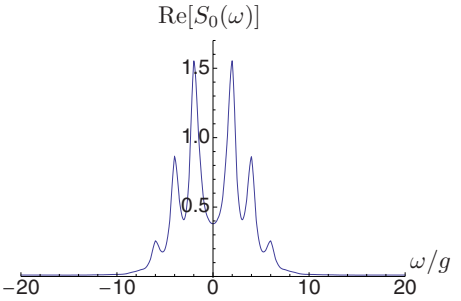

FIG. 10. (Color online) Real part of $S_0(\omega)$ for the superfluid state $|\psi_{\text{SF2}}\rangle$ with a total number of eight atoms and $d=\lambda/4$.

binomial distribution. Figure 12, which plots the FWHM w of the physical spectrum as a function of σ, shows as expected a linear dependence, further illustrating the use of that spectrum in helping to characterize the many-body state of the atomic system.

V. ENTANGLEMENT

In this section we make some brief remarks on the entanglement generated between the light fields and the atoms, and its dependence on the state on the atomic system. We characterize the entanglement in terms of the logarithmic negativity [17]

$$E_{\mathcal{N}}(\rho) = \log_2 \|\rho^{T_A}\|_1, \tag{21}$$

where ρ^{T_A} is the partial transpose of ρ and $\|\cdot\|_1$ denotes the trace norm.

There is always some ambiguity in the way a quantum system is described in terms of its subsystems. One simple way to describe the system at hand is as a four-partite system comprised of two optical modes and the atoms in the two wells. It is then possible to trace over any two parts of the full system, and to consider the remaining subsystems only. We find that independently of our choice of the subsystems being considered, the resulting reduced density operator does not retain any trace of whatever entanglement may have characterized the full system. This leads us to describe instead the full system as a bipartite system, the two subsystems being the optical field and the atoms.

The situation is particularly simple if the atomic system is initially in a product of Fock states. As discussed in Sec. III, in the absence of quantum jumps between the times 0 and t we have

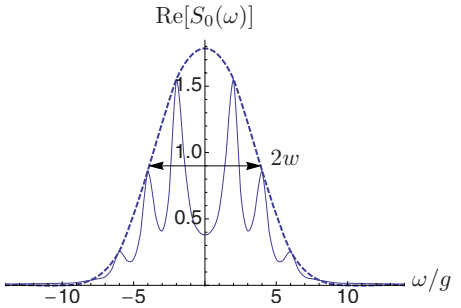

FIG. 11. (Color online) The envelope and FWHM.

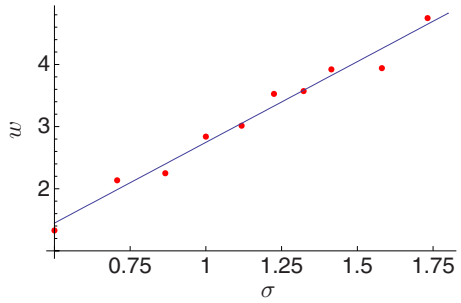

FIG. 12. (Color online) FWHM w vs atomic number uncertainty of each well σ. The data points correspond to $N=1$, 2, 3, 4, 5, 6, 7, 8, 10, and 12. The straight line is the fit to the data points.

$$|\psi(t)\rangle = |\alpha_k(n_0,n_1,d,t),\alpha_{-k}(n_0,n_1,d,t);n_0,n_1\rangle, \quad (22)$$

where the amplitudes of the coherent states α_k and α_{-k} depend on the atomic populations of the wells and on their separation. It is immediately apparent from Eq. (22) that the total optical field is not entangled with the atoms. As previously remarked, for coherent states quantum jumps do not affect the light field. Hence $|\psi(t)\rangle$ is always a product state for this four-partite system; that is, no entanglement builds up between the atoms and the field.

The situation is markedly different for atoms in a superfluid state. For example, in the atom number-conserving approximation $|\psi_{SF2}\rangle$, and in the absence of quantum jumps between times 0 and t, the state of the system at time t is

$$|\psi(t)\rangle = \sum_{n_0}^{N} b_{n_0}|\alpha_k(n_0,d,t),\alpha_{-k}(n_0,d,t);n_0,N-n_0\rangle, \quad (23)$$

a state for which the light field and atoms are clearly entangled. Dissipation and the associated quantum jumps clearly impact the amount of entanglement in that case. To illustrate that point, we first evaluate the logarithmic negativity of the bipartite atom–optical field system for a well separation of $d=\lambda/4$ while neglecting pump and decay mechanisms. In that case, from Eqs. (3) and (5) the system is described by the Hamiltonian

$$\hat{H} = \hbar g[(\hat{n}_0+\hat{n}_1)(\hat{a}_k^\dagger\hat{a}_k+\hat{a}_{-k}^\dagger\hat{a}_{-k})+(\hat{n}_0-\hat{n}_1)(\hat{a}_{-k}^\dagger\hat{a}_k+\hat{a}_k^\dagger\hat{a}_{-k})], \quad (24)$$

and we find easily that

$$|\psi(t)\rangle = \sum_{n_0}^{8} \beta_{n_0}|\alpha_k(n_0,t),\alpha_{-k}(n_0,t);n_0,N-n_0\rangle,$$

where

$$\alpha_k(n_0,n_1,t) = \frac{\alpha}{2}(e^{-2ign_0t}+e^{-2ign_1t}),$$

$$\alpha_{-k}(n_0,n_1,t) = \frac{\alpha}{2}(e^{-2ign_0t}-e^{-2ign_1t}). \quad (25)$$

The logarithmic negativity $E_{\mathcal{N}}$ corresponding to that case is shown in Fig. 13 for $N=8$ atoms. We observe that $E_{\mathcal{N}}=0$ for $t=\ell\pi/g$, where ℓ is an integer, indicating the absence of entanglement between the light and the atoms. These are the times when the atoms do not scatter any light into the $-k$ mode, and the state of the system has undergone a full revival to its original, unentangled form.

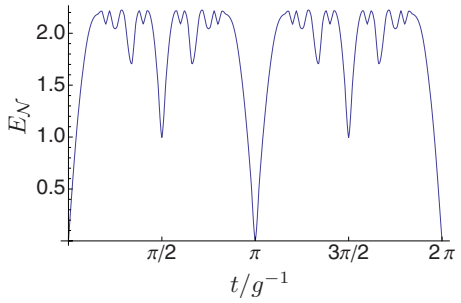

FIG. 13. (Color online) Logarithmic negativity of light and atoms for a perfect cavity (no decay and no pump). The initial coherent amplitude of k mode $\alpha=1$ and atoms are in superfluid states $|\psi_{SF2}\rangle$ with total number of atoms $N=8$ and well separation $d=\lambda/4$.

The situation is changed when including the external pump in the description of the system, in which case there is no longer an exact revival. Figure 14 illustrates that a remnant of that feature is still observable in this case, but it disappears almost completely when both pump and dissipation are included; see Fig. 15. In that latter case, the entanglement between the light field and the atoms disappears completely over time as would be expected.

As a final point, we remark that similar results hold in case the superfluid atomic system is described by the state $|\psi_{SF1}\rangle$, although the maximum value of the logarithmic negativity is now larger, due to the larger number of terms in the expansion of that state in terms of number states.

VI. CONCLUSIONS

We have studied the interaction of a light field and ultracold atoms trapped in a two-well optical potential in a lossy cavity. We have calculated the reflected intensity, the physical spectrum, and the logarithmic negativity, and shown that all three observables present completely different features for

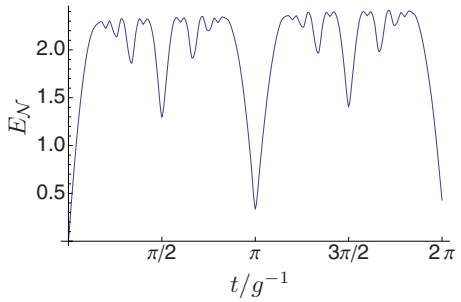

FIG. 14. (Color online) Logarithmic negativity for a perfect cavity, without decay but including the pump. The initial coherent amplitude of the k mode is $\alpha=1$ and the atoms are initially in the superfluid state $|\psi_{SF2}\rangle$ with total number of atoms $N=8$ and well separation $d=\lambda/4$. The pump constant is $\eta=0.5g$.

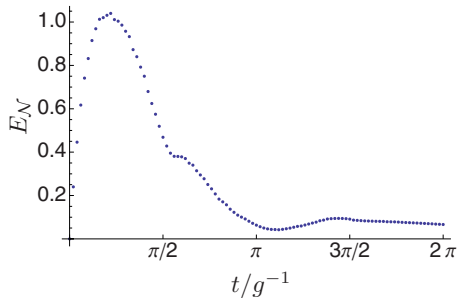

FIG. 15. (Color online) Logarithmic negativity including dissipation. The initial coherent amplitude of the k mode is $\alpha=1$ and the atoms are in a superfluid state $|\psi_{\mathrm{SF2}}\rangle$ with total number of atoms $N=2$ and well separation $d=\lambda/4$. The pump constant is $\eta=0.2g$ and the decay constant is $\gamma=0.7g$. The curve has been averaged over 100 trajectories.

the two different many-body atomic states, allowing one to distinguish these states.

Our explicit results are for small systems of a few atoms only, and a legitimate question is to ask to which extent this scheme remains practical for larger numbers of atoms and/or of wells. Returning, for instance, to the physical spectrum of the system, it is clear that the interpretation of the results becomes increasingly complicated in that case: the superfluid spectrum in Fig. 10 rapidly acquires additional peaks corresponding to all allowed values of $|2n_0-N|$, odd or even depending on the well separation. In the Fock states situation, though, the physical spectrum will still be characterized by two peaks only as in Fig. 8, so the distinction between the superfluid and Fock states situations should still be observable. However, the distinction between the two superfluid descriptions is expected to become more difficult to make as the number of particles in increase.

Going from two to multiple wells is also worth considering. For instance, for a well separation $d=\lambda/4$ the contributions to the backscattered light alternatively add and subtract [see Eq. (10)], thereby masking the double-peak signature in the physical spectrum. Even for $d=\lambda/2$, where this difficulty is absent, well-to-well fluctuations in atomic numbers result in a situation more akin to the case of a superfluid. This, of course, would not be the case for a perfect Mott insulator state, where the atom number in each well is precisely the same. We also note that experiments normally involve an additional harmonic trap superimposed onto the optical lattice, leading, for instance, to a "wedding cake" distribution of atomic populations. While our scheme is in principle able to distinguish the appearance of such structures, its experimental implementation is bound to be challenging. As such, our considerations are of most relevance for experiments involving small atom-cavity systems.

Future work will generalize this analysis to more complex many-body atomic states, using in particular Laguerre-Gaussian modes of the light field to characterize the state of vortex lattices. We are also extending this work to optomechanical situations, using radiation pressure force on Fabry-Pérot resonators with moving mirrors to induce quantum phase transitions and monitor them optically in real time.

ACKNOWLEDGMENTS

We thank D. Meiser and M. Bhattacharya for stimulating discussions. This work was supported in part by the U.S. Office of Naval Research, by the National Science Foundation, and by the U.S. Army Research Office.

[1] M. Lewenstein, A. Sanpera, V. Ahufinger, B. Damski, A. Sen, and U. Sen, Adv. Phys. **56**, 243 (2007).
[2] M. Greiner, O. Mandel, T. Esslinger, T. W. Hänsch, and I. Bloch, Nature (London) **415**, 39 (2002).
[3] M. Greiner, O. Mandel, T. W. Hänsch, and I. Bloch, Nature (London) **419**, 51 (2002).
[4] T. Rom, T. Best, O. Mandel, A. Widera, M. Greiner, T. W. Hänsch, and I. Bloch, Phys. Rev. Lett. **93**, 073002 (2004).
[5] T. Stoferle, H. Moritz, K. Gunter, M. Kohl, and T. Esslinger, Phys. Rev. Lett. **96**, 030401 (2006).
[6] G. Thalhammer, K. Winkler, F. Lang, S. Schmid, R. Grimm, and J. H. Denschlag, Phys. Rev. Lett. **96**, 050402 (2006).
[7] D. Jaksch, V. Venturi, J. I. Cirac, C. J. Williams, and P. Zoller, Phys. Rev. Lett. **89**, 040402 (2002).
[8] D. Jaksch, C. Bruder, J. I. Cirac, C. W. Gardiner, and P. Zoller, Phys. Rev. Lett. **81**, 3108 (1998).
[9] D. Jaksch and P. Zoller, Ann. Phys. (N.Y.) **315**, 52 (2005).
[10] J. J. Garcia-Ripoll, M. A. Martin-Delgado, and J. I. Cirac, Phys. Rev. Lett. **93**, 250405 (2004).
[11] T. Miyakawa and P. Meystre, Phys. Rev. A **73**, 021601(R) (2006).
[12] N. Barberán, M. Lewenstein, K. Osterloh, and D. Dagnino, Phys. Rev. A **73**, 063623 (2006).
[13] I. B. Mekhov, C. Maschler, and H. Ritsch, Nat. Phys. **3**, 319 (2007); I. B. Mekhov and H. Ritsch, Phys. Rev. Lett. **102**, 020403 (2009).
[14] W. Chen, D. Meiser, and P. Meystre, Phys. Rev. A **75**, 023812 (2007).
[15] K. Mølmer, Y. Castin, and J. Dalibard, J. Opt. Soc. Am. B **10**, 524 (1993).
[16] J. H. Eberly and K. Wódkiewicz, J. Opt. Soc. Am. **67**, 1252 (1977).
[17] G. Vidal and R. F. Werner, Phys. Rev. A **65**, 032314 (2002).
[18] L. Salasnich, A. Parola, and L. Reatto, Phys. Rev. A **60**, 4171 (1999).
[19] G. J. Milburn, J. Corney, E. M. Wright, and D. F. Walls, Phys. Rev. A **55**, 4318 (1997); J. Ruostekoski and D. F. Walls, *ibid.* **58**, R50 (1998); J. Ruostekoski, *Lecture Notes in Physics: Directions in Quantum Optics*, edited by H. H. Carmichael, R. J. Glauber, and M. O. Scully (Springer, Berlin, 2001).
[20] J. M. Zhang, W. M. Liu, and D. L. Zhou, Phys. Rev. A **77**, 033620 (2008).
[21] J. F. Corney and G. J. Milburn, Phys. Rev. A **58**, 2399 (1998).
[22] R. J. Glauber, Phys. Lett. **21**, 650 (1966).